Effective Conductivity Modeling of a Fluid Saturated Porous Rock

Xin Zhan, M. Nafi Toksöz
Earth Resources Laboratory
Dept. of Earth, Atmospheric and Planetary Sciences
Massachusetts Institute of Technology
Cambridge, MA , 02139

May 27, 2007

Abstract

The microstructure of a porous medium and physical characteristics of the solid and the fluids that occupy the pore space determine the macroscopic transport properties of the medium. The computation of macroscopic properties from the rock microtomography is becoming an increasingly studied topic. The transport properties are especially difficult to determine at the microscopic scale. In this paper, we will focus on modeling the electric conductivity from the X-ray CT microtomograhpy of a $1mm^3$ Fontainbleau Sandstone sample. To accomplish this, we modified the finite difference Laplace solver developed at NIST (National Institute of Standards and Technology, Gaithersburg, MD 20899-8621, U.S.A). Our modified finite difference code can calculate the effective conductivity of random materials with different levels of conductivity contrasts. The effective conductivity and the current density distribution of gas, oil and different salinity brine saturated Fontainbleau Sandstone are calculated using a two-phase model. When we compare our numerical results with experimental results from previous studies, the numerically resolved conductivity is almost 100% lower than the experimental data. This is the case for all of the previous work on the numerical computation of electric conductivity from digital images of rocks. Our explanation for this large discrepancy is due to the exclusion of the surface conductivity in the electric double layer (EDL) at the rock-electrolyte interface. Thus, we develop a three phase conductivity model to include the surface conductivity and determine the effective conductivity of the numerical grids containing the EDL from the Waxman-Smits equation. By adding the surface conductivity into our numerical modeling, the calculated conductivity from rock microtomography is much closer to the experimental data.

1. Introduction

Understanding the interaction between rock, pore space and pore fluids in the microscopic scale is crucial to better interpretation of macroscopic geophysical measurements. With the development of modern imaging techniques, such as advanced X-ray CT and laser confocal microscopy, one can directly image the 3D pore structure of sedimentary rock at micrometer resolution (Coles et al., 1994;

Hazlett, 1995; Coles et al., 1996; Pal et al., 2002). Meanwhile, with the advance in computational techniques, it is now possible to compute transport properties such as permeability and electric conductivity on large three dimensional systems.

Recently, computation of permeability (Alder et al., 1990; Pal et al., 2002) and electric conductivity (Alder et al., 1990; Arns et al., 2002; Pal et al., 2002) on the 3-D micro X-ray computed microtomography have been increasingly studied. Laboratory measurements of dc electric conductivity are also made over a wide range of porosities. However, the numerically calculated conductivities that are found by treating the fluid saturated porous medium as a two-phase material are consistently lower than experimental data. The current explanation for this discrepancy is mostly described by the percolation differences between model and real materials (Adler, 1992; Bentz et al., 1994). The insufficient sampling volume of microtomography images could also be responsible for the discrepancy.

In this paper, we propose a new three-phase numerical conductivity model for the fluid saturated porous media as an effective means to minimize the difference between numerical and experimental results for the effective conductivity. Besides the traditional two-phase model where rock matrix is considered to be phase one and pore fluid to be phase two, we add the third phase which is the bound fluid at the grain fluid interface to the model. The purpose of including this third phase is to study the effect of surface conductivity on the total effective conductivity. Surface conductivity within the electric double layer can contribute substantially to the effective electrical conductivity of the porous medium (Revil et al., 1997).

We make the effective conductivity computation on a digitized CT image of the Fontainbleau Sandstone sample with 7.37% porosity. The numerically obtained conductivity by modeling the fluid saturated porous medium as a two-phase material from rock CT microtomograhpy is almost 100% lower than the experimental data. The large discrepancy between the numerical and experimental result was thought to be the insufficient sampling volume and limited resolution of the digitized CT image. We come up with another possible explanation to this discrepancy, which is due to the exclusion the surface conductance. In our study, instead of modeling the fluid saturated porous rock as a two-phase material, we introduce the third phase which is the electric double layer (EDL) at the solid-fluid interface. By adding the third phase with the surface conductivity, the numerically calculated conductivity can increase by 5%-200% depending on the salinity of the saturating fluid. This dramatic increase by adding the surface conductivity can minimize the difference between numerical and experimental conductivity results to a large extent.

To solve the problem of computing the effective conductivity for disordered materials numerically, we based our study on the industry-standard finite difference (FD) code developed at NIST (National Institute of Standards and Technology, Gaithersburg, MD 20899-8621, U.S.A). We modified the code to handle different conductivity contrast levels between the solid grain and the saturating phase, and try to minimize the numerical instability. We calculate the effective conductivity of the Fontainbleau Sandstone sample saturated with gas, oil and saline water with conductivity ranging from 10^{-5} S/m to 10 S/m. We also compare the numerical results with an empirical formula, Archie's law, for the saline water saturations. The numerically obtained conductivity by setting the quartz conductivity as 10^{-12} S/m and the fluid conductivity between 10^{-5} S/m and 10 S/m agrees well with Archie's law. We also

compare our numerical result with a previous Ph.D thesis study by Arns (Arns, 2001). Arns models water saturated Fontainbleau Sandstone as a simple two phase material with 1:0 contrast through a porosity range of 5% - 25%. Our numerically calculated formation factor, which is the ratio between the effective conductivity of the fluid saturated porous medium and fluid conductivity, is very close to his result at 7.99% porosity.

However, when we compare our numerical solution and Arns' numerical result with the experimental data in his Ph.D thesis at 7%-8% porosity range, the numerical solution of the formation factor is almost 100% lower than the experimental result. The difference between the numerical and experimental result was thought to be finite size effects, discretization errors and statistical fluctuations (Arns, 2001). We extend our numerical model from the simple two-phase model with different contrast levels to a three-phase model by introducing the EDL at the solid-fluid interface. We redefine our FD model to have three kinds of grid cells. The grid cells that correspond to grain and pore space are the same as the two-phase model. In addition, we search for all the grid cells located at the grain-pore space boundary and define them to be the third kind of grid cell. Surface conductivity is always higher than the free electrolyte conductivity in the pore space, which means that the boundary cells have higher conductivity than the pore space grid cells. We then recalculate the effective conductivity of the fluid saturated Fontainbleau Sandstone sample using the three phase conductivity model. Also, we treat the surface conductivity as a function of electrolyte conductivity to study the effect of surface conductivity in different salinity environments. The calculated conductivity from the three phase model is much closer to the experimental data compared with the two phase numerical results.

2. Effective conductivity of porous medium and Finite Difference Implementation

The effective dc conductivity of a random material can be solved by Ohm's Law,

$$\vec{J}(r) = \sigma(r)\vec{E}(r). \tag{1}$$

The conductivity value σ of a composite n-phase material is a function of location r. For a steady state conductivity problem, where the currents are steady in time, the charge conservation equation,

$$\nabla \cdot \vec{J} + \frac{\partial \rho}{\partial t} = 0 \tag{2}$$

reduces to

$$\vec{\nabla} \cdot \vec{J}(r) = -\vec{\nabla} \cdot (\sigma(r) \cdot \vec{\nabla} V(r)) = 0. \tag{3}$$

Between phases having different conductivities, the boundary conditions require that the current density normal to the interface and the potential are continuous. We can calculate the macroscopic conductivity of the random material by applying an electric potential gradient across the sample. The volume

averaged current density can be used to compute the effective conductivity from Ohms' law, as given in equation (1).

To calculate the dc effective conductivity of the porous medium, we employ an industry standard finite difference (FD) code developed at NIST (National Institute of Standards and Technology, Gaithersburg, MD 20899-8621, U.S.A). The FD code solves the Laplace equation in the finite difference form with given boundary conditions using a conjugate gradient solver (Garboczi, 1998). As for the material properties, finite difference electrical conductivity programs can handle arbitrary diagonal conductivity tensors. The conductivity tensor $\sigma(r)$ is defined for each phase in the microstructure as a function of location. The 3D microstructure is redefined to a 1D label to be taken in the finite difference scheme. We can define an electric potential gradient across the sample in x, y, and z directions respectively and calculate the current density in all three directions at every location within the microstructure. By doing the volume average of the local current densities, we can back out the full conductivity tensor as indicated in Fig 1. There is an intrinsic challenge solving Laplace's equation when the conductivity contrast between the different phases is very high. For our specific problem, the solid matrix is defined to be quartz with the conductivity of 10^{-12} S/m. As for the fluid phase, we want to have a conductivity range between 10^{-5} S/m and 10 S/m. Thus, the contrast between the two phases could be 7 to 13 orders in magnitude. To handle such a large contrast, we start from the low conductivity contrast and gradually relax the potential field, then gradually increase the conductivity contrast to make the result converge. We use a relatively loose convergence criteria for the gradient of the electric energy when the conductivity contrast is small. Then, we apply a more strict criteria when we reach our target contrast level to make sure we run enough conjugate gradient cycles to make sure that the gradient is no longer changing.

To validate the finite difference code, we apply the code to a simple geometry and compare the numerically calculated conductivity with an analytic solution. We also compare the current density distribution from the FD code with the result from a commercial finite element software package, FEMLAB. The geometry we use is a spherical inclusion with a radius of 15 meters in the center of a 100 meter cube as shown in Fig 2. The spherical inclusion is defined to be phase 1 and cube host is defined to be phase 2. The volume fraction of the spherical inclusion is f_1= 0.007153, the conductivity of the sphere is $\sigma_1 = 10^{-5}$ S/m, and the conductivity of the cubic host is σ_2 = 0.06S/m. The analytic solution for a two-component material with spherical inclusion can be calculated by the Clausius-Mossotti formula

$$\frac{\sigma^* - \sigma_2}{\sigma^* + 2\sigma_2} = f1\frac{\sigma_1 - \sigma_2}{\sigma_1 + 2\sigma_2}. \qquad (4)$$

The difference between the FD calculated conductivity by applying a unit electric field of 1V/m in the x-direction across the cube and the Clausius-Mossotti formula is only 0.25%. We also display a slice view of the distribution of the current density in the x-direction and compare with the FEMLAB result in Fig 3. The color bar represents the absolute value of the current density in the direction of the electric potential gradient.

3. Numerical results of oil, gas and saline water saturation

We next apply the FD code on our Fontainbleau Sandstone CT microtomographic sample. The digitized sample we have is a 200^3 binary voxel. The pore space is coded to be '0' and grain material to be '1'. The voxel is close to a cube-shape with the resolution of 4.68 x 4.68 x 5.21 microns in X, Y and Z direction respectively. The whole sample is 1mm^3 in volume with 7.37% porosity, as shown in Fig 4. In Fig 4, the left hand image shows the scan with pore space rendered transparent while the right hand image shows the result if the grain material is eliminated, a "pore cast".

In past studies, people treat the solid matrix as an insulator and use 0 for the grain conductivity. In our calculation, the grain is considered to be quartz with the conductivity of 10^{-12} S/m instead of 0. We saturate the Fontainbleau Sandstone with gas, oil and saline water with different values of salinity. For the saturation phase, we also use a realistic conductivity value instead of using 1 as a normalized conductivity, as was done in the previous studies. The conductivity values for different saturating phases are listed in the second row of Table 1. The Fontainbleau Sandstone is digitized to be a binary voxel image at this stage. We assign all the '0's in the sample, which stands for the pore space, with the saturating phase conductivity and all the '1's with the quartz conductivity. The effective conductivity of the saturated Fontainbleau Sandstone is listed in the last row of Table 1. For the saline water saturation, the numerically calculated effective conductivity agrees well with the empirical Archie equation (Archie, 1942). Archie suggests that the conductivity of fluid saturated rock is proportional to the fluid conductivity, and introduces the formation factor F as $F = \dfrac{\sigma_f}{\sigma_{rock}}$. Archie's equation is usually written as

$$F = \frac{\sigma_f}{\sigma_{rock}} = \phi^{-m}. \qquad (5)$$

The cementation exponent, m ,is dependent on the lithology.

To visually represent the sandstone saturated with different fluids, we also display the current density distribution in a common (base 10) logarithm. Fig 5 to Fig 7 correspond to the gas, oil and saline water saturations, respectively. From the current density distribution, we can resolve the pore space very well which corresponds to the hot spots in the map. With an increase of the conductivity contrast between the saturation phase and host grain phase, the boundary between the pore space and grain becomes sharper. It is obvious that larger contrasts can better resolve the details of the structure.

By applying the electric potential gradient in the x, y and z direction, we can get the volume averaged current density in all three dimensions. Then using Ohm's law in equation (1), the full 3×3 conductivity tensor can be obtained. The conductivity tensor with the 10^{-4}S/m saline water saturation is

$$\begin{bmatrix} \sigma_{xx} & \sigma_{xy} & \sigma_{xz} \\ \sigma_{yx} & \sigma_{yy} & \sigma_{zz} \\ \sigma_{zx} & \sigma_{zy} & \sigma_{zz} \end{bmatrix} = \begin{matrix} 3.2479\text{e}^{-7} & 2.8427\text{e}^{-8} & 2.7608\text{e}^{-8} \\ [3.6354\text{e}^{-8} & 2.9465\text{e}^{-7} & 2.7758\text{e}^{-8}] \\ 3.3375\text{e}^{-8} & 2.5638\text{e}^{-8} & 3.0125\text{e}^{-7} \end{matrix}$$

Note that the diagonal elements in the conductivity tensor are one order larger than the off-diagonal

elements. From the conductivity tensor, we can see that our Fontainbleau Sandstone sample is relatively isotropic. We can back out the formation factor by calculating the ratio between a range of fluid conductivity values as indicated in Table 1 and saturated rock conductivity from equation (5).The formation factor we get is 0.003223, which is similar to the 0.003172 obtained by Arns (Arns, 2001) on a 7.99% porosity Fontainbleau Sandstone CT image. We superimpose our result on the figure from the Arns paper in Fig 8. Our estimation of the cementation exponent in the formation factor of the Fontainbleau Sandstone sample using Archie's law (5) is m = 2.2 compared with his result of m = 2.28. The green square in Fig 8 is our estimation of the formation factor with an error bar indicating the standard deviation on it. The black squares are the numerically calculated formation factor by Arns and the black spheres are the experimental data. Clearly, both our numerical calculated conductivity and Arns' numerical result using the two-phase model is almost 100% lower than the experimental measured conductivity.

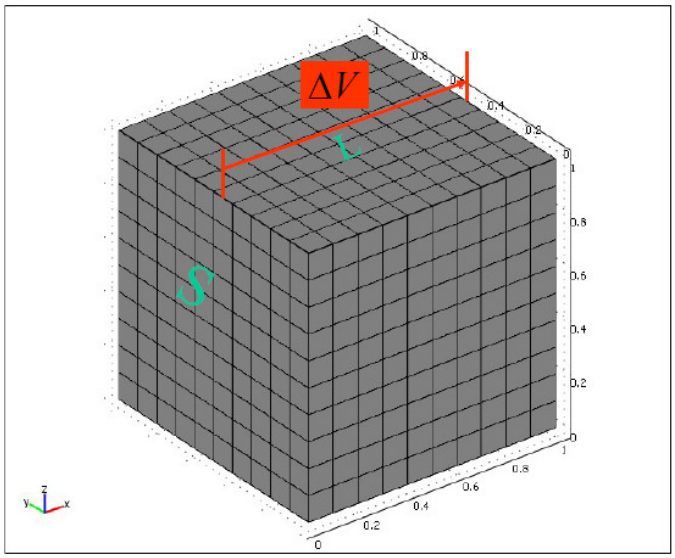

$$\sigma_{eff} = (\frac{L}{\Delta V})\frac{1}{A}\iint_S \sigma(r)(-\hat{x}\cdot\vec{\nabla}V)dS$$

Figure 1: Effective conductivity calculation of a random material using the finite difference scheme.

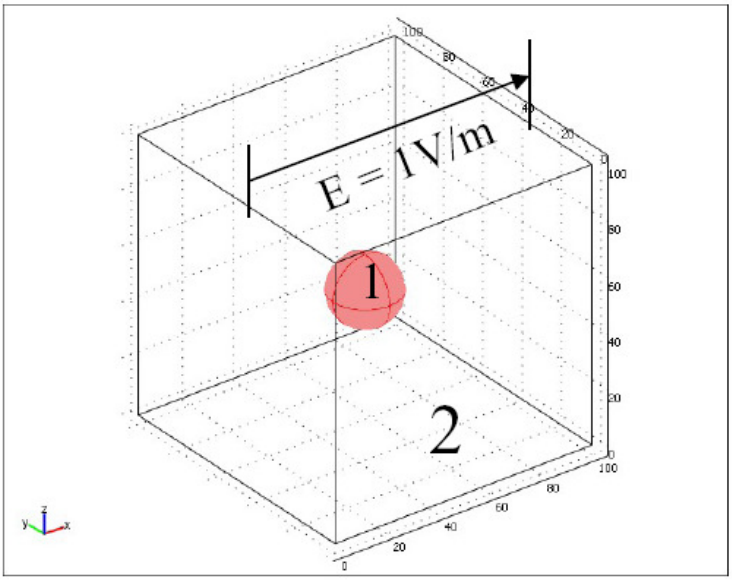

Figure 2: The geometry of a spherical inclusion (phase 1) in a cubic host (phase 2). An electric potential gradient of 1 V/m is applied in x-direction.

Saturation Phase	**Gas**	**Oil**	**Saline Water**						
Saturation Conductivity (S/m)	1e-11	5e-9	1e-5	1e-4	1e-3	1e-2	1e-1	1	10
Effect Conductivity (S/m)	7.016e-12	1.128e-9	Archie's Law						

Table 1: The conductivity of gas, oil and saline water as saturation phase and the effective conductivity of the saturated Fontainbleau Sandsonte.

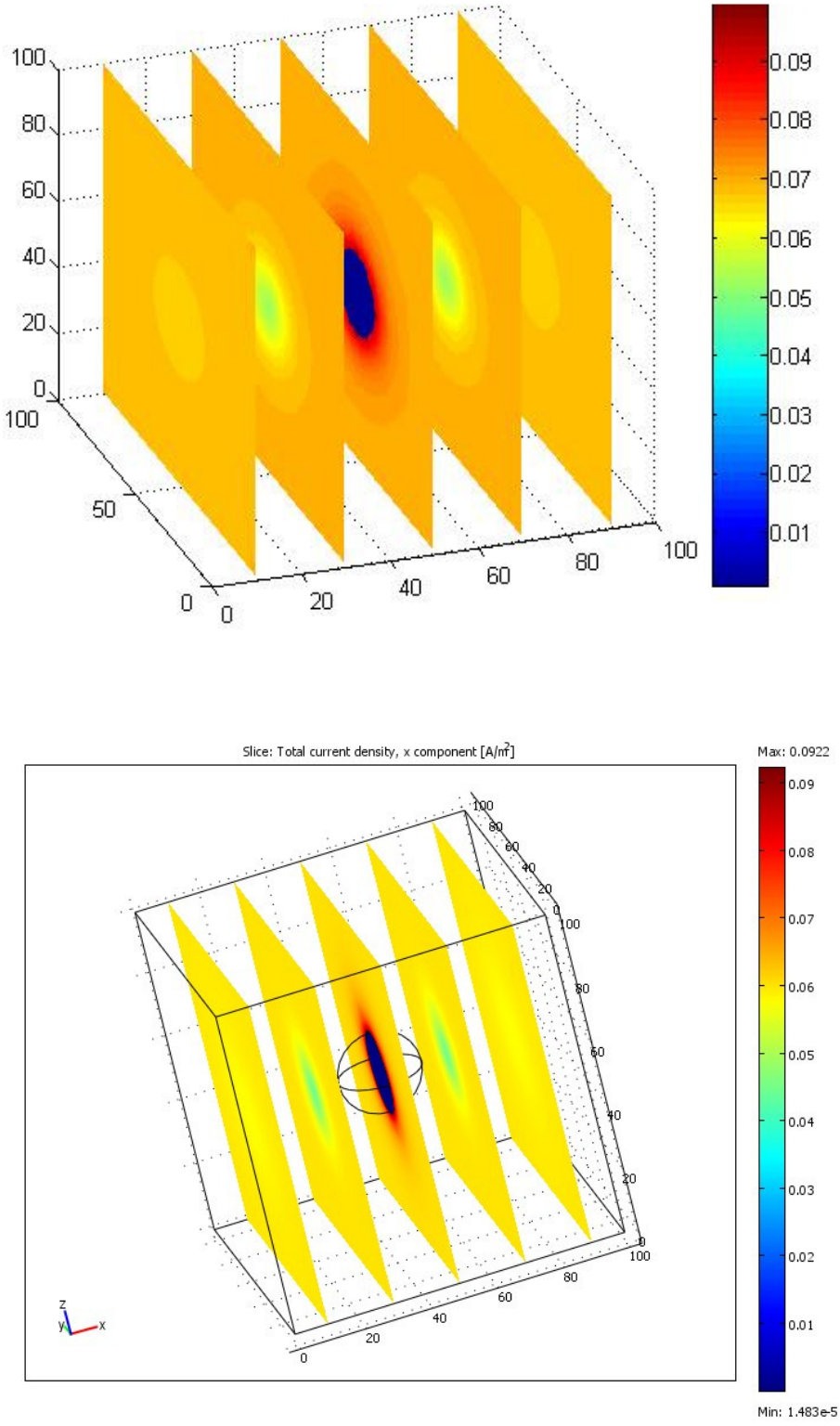

Figure 3: The current density distribution of the spherical inclusion in a cubic host Color bar indicates the magnitude of the current density. Above is the FD result and below is the FEMLAB result.

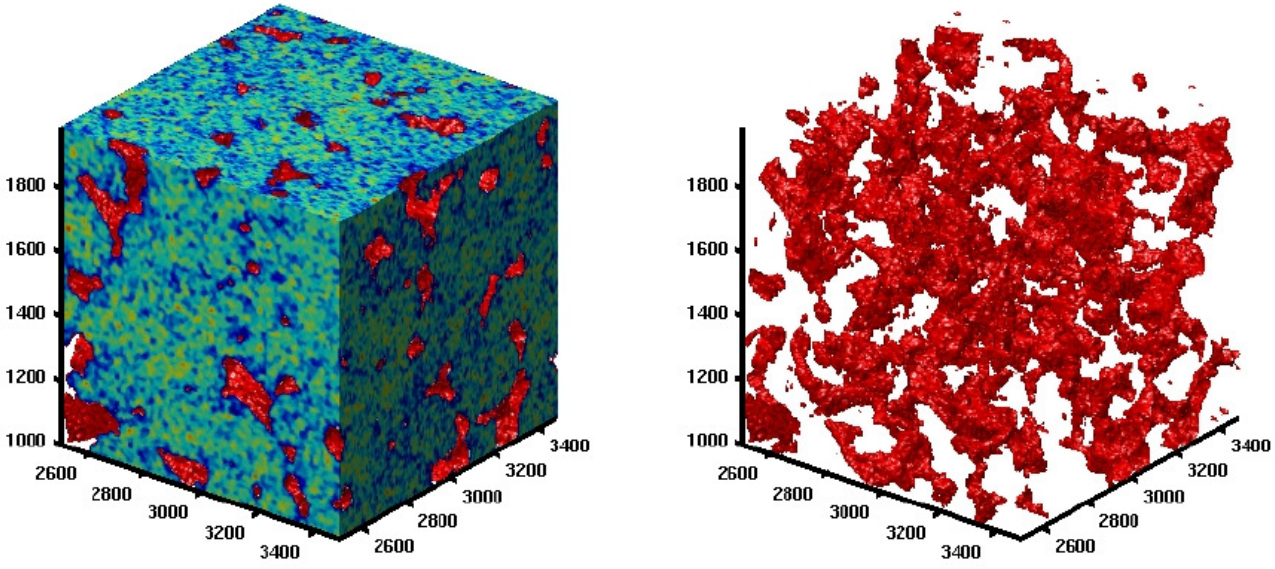

Figure 4: The Fontainbleau Sandstone CT microtomogrphay. On the left panel, the red indicate the pore space and the blue indicate the grain. On the right panel, the grain space is eliminated and remain a ‘pore cast’.

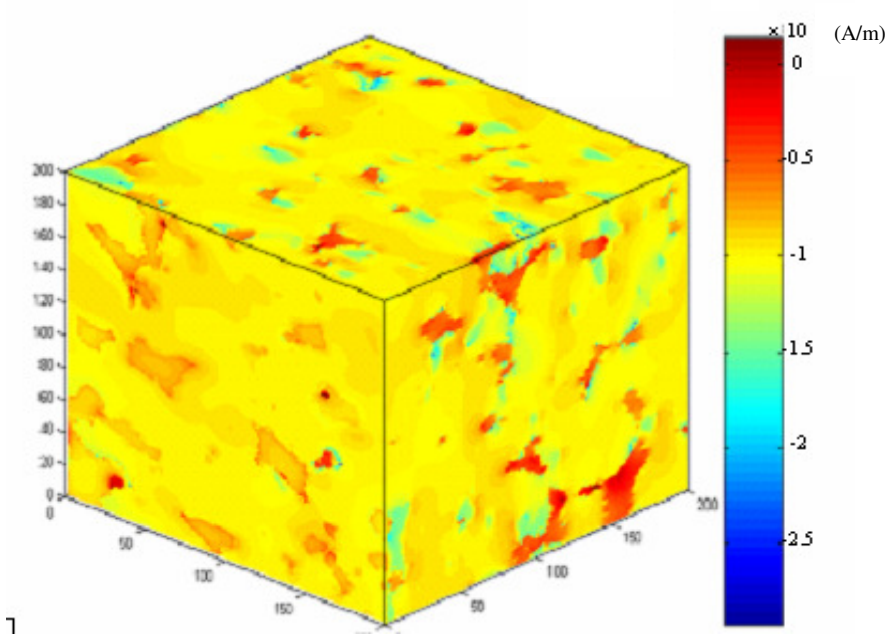

Figure 5: The current density distribution when Fontainbleau Sandstone saturated with gas. The color bar indicated the common (base 10) logarithm of the current density.

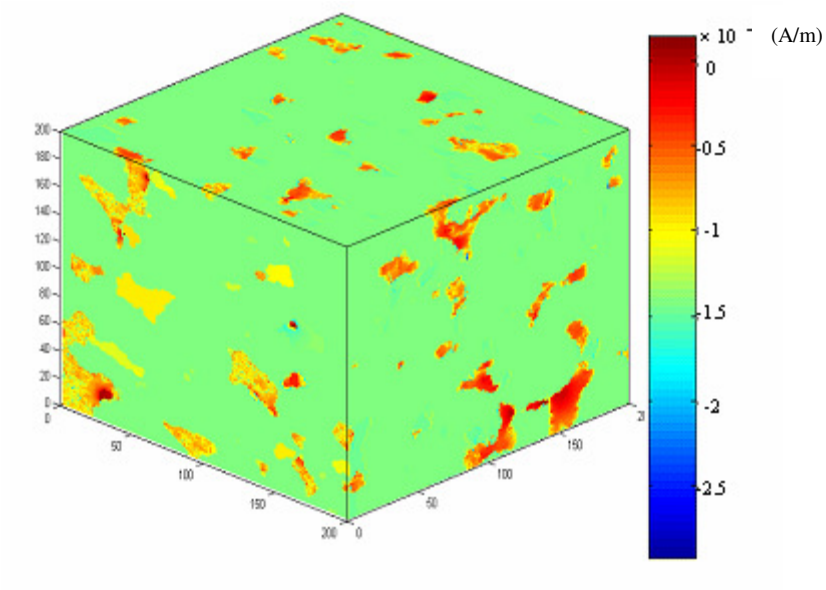

Figure 6: The current density distribution when Fontainbleau Sandstone saturated with oil. The color bar indicated the common (base 10) logarithm of the current density.

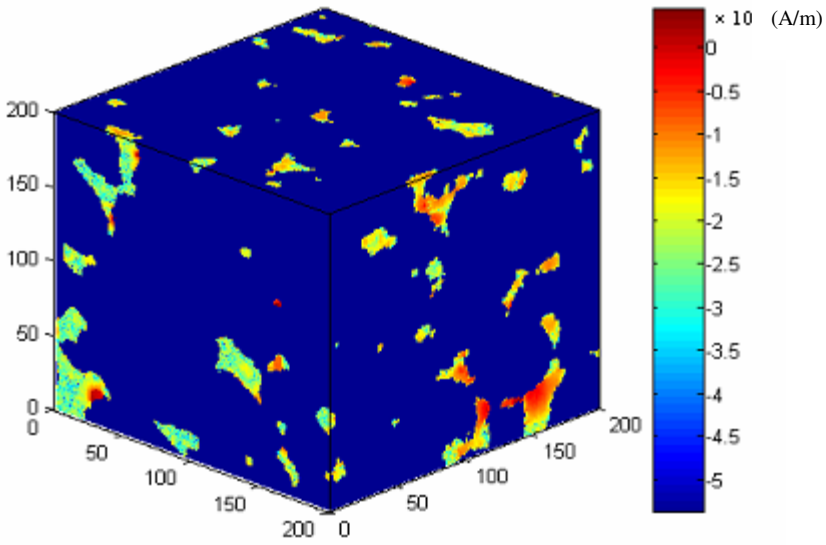

Figure 7: The current density distribution when Fontainbleau Sandstone saturated with saline water with the conductivity of 10^{-5} S/m. The color bar indicated the common (base 10) logarithm of the current density.

We know that when a fluid electrolyte comes into contact with a neutral solid surface, anions from the electrolyte are chemically adsorbed to the wall leaving behind a net excess of cations distributed near the wall. The region is known as the electric double layer (EDL) (Pride and Morgan, 1991). The thickness of the EDL is defined as the Debeye length, and is in the nano-meter range. The first layer of cations is bound to the anion / solid surface. Beyond this first layer of bound cations, there is a diffuse distribution of mobile cations whose position is determined by a balance between electrostatic attraction to the adsorbed layer and diffusion toward the neutral electrolyte. The separation between the mobile and immobile charge is called the shear plane. The zeta potential, ζ, is the electric potential at the shear plane, and the electric potential in neutral electrolyte (no excess charge) is defined to be zero (Pride and Morgan, 1991; Bockris and Reddy, 2000). The surface conductivity within this electrical diffuse layer (noted as EDL) can contribute substantially to the effective conductivity of the porous medium (Revil et al., 1997).

Using the two-phase model to calculate the effective conductivity of the fluid saturated rock excludes the contribution from the surface conductivity. For the experimental case when we saturate the rock with electrolyte, the EDL at the fluid-grain is naturally present. The effective conductivity measured from the experiment therefore includes the surface conductivity in the EDL.

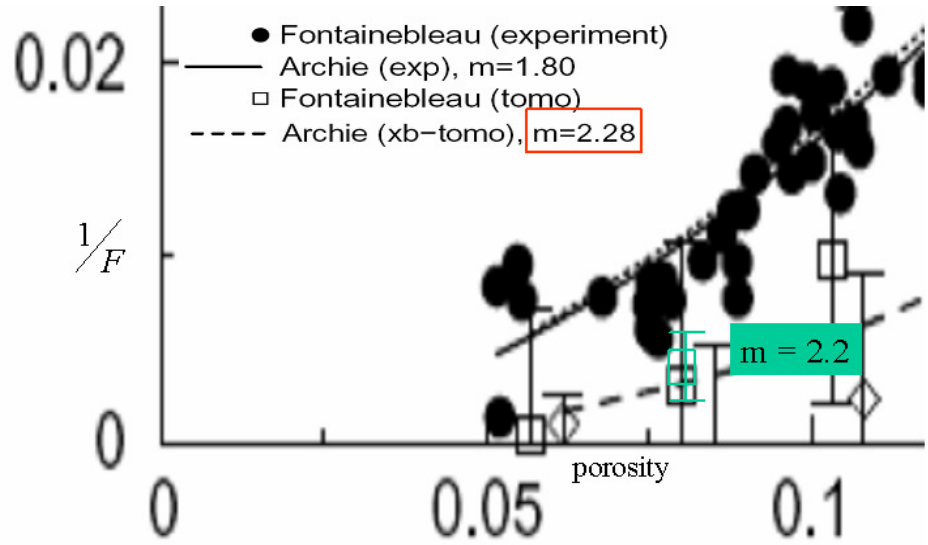

(Arns, 2001, PhD thesis)

Figure 8: The comparison between our numerical calculated formation factor with the Arns's result. The green square is our formation factor and black squares are the Arns's result with two-phase model. The black spheres are the experiment measurements.

Our effort is to numerically model the effect of larger values of conductivity that exist close to the grain surface than in the bulk pore fluid. We extend our numerical model from two-phase to three-phase to account for the EDL at the solid -fluid interface. The thickness of the EDL (χ_d) is at the nano-meter scale and the Fontainbleau Sandstone is a $1mm^3$ cube. With current computer power, it is extremely difficult to discretize a mili-meter cube on the nano-meter scale. The storage required by the nano-meter grid will be very large. We are therefore limited to using the 5 micron grid (L), which is the same as the resolution of our CT image voxel. We define all of the grid cells at the pore-grain boundary to be the third kind of cell, and change the numerical representation of the porous rock from binary cube to a three phase cube as illustrated in Fig 9. In the three phase conductivity model, the first kind of grid cell has the conductivity of σ_1 equal to the quartz conductivity. The second kind of grid cell has the conductivity of σ_2 equal to the free electrolyte conductivity in the pore space. The third kind of grid cell is the boundary grid containing an EDL at fluid-solid interface with the conductivity σ_3. The conductivity distribution in the third kind of grid cell is illustrated in Fig 10. We calculate σ_3 by integrating the larger surface conductivity σ_{surf} over the double layer thickness χ_d, and geometrically average this with σ_2 in the remainder of the boundary grid cell (L-χ_d).

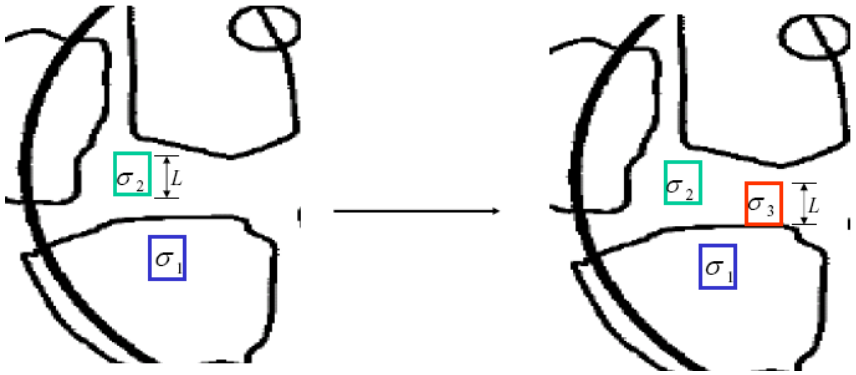

Figure 9: Two-phase representation of the porous rock (left) and three-phase representation of the porous rock (right). Both model has the same size of grids (L).

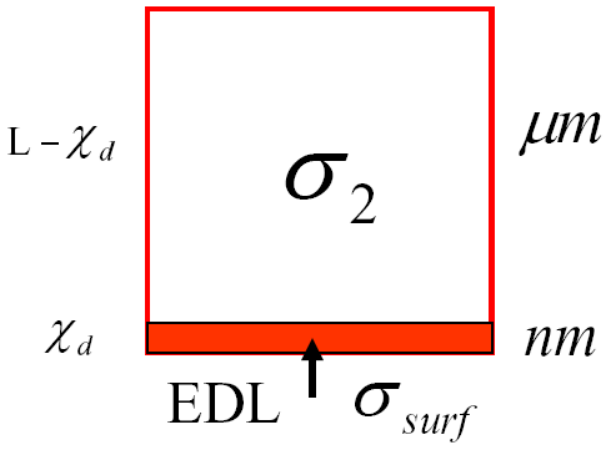

Figure 10: The conductivity distribution in the third kind of grid of length L with conductivity σ_3. A thin electric double layer (EDL) with length χ_d is include in the grid with conductivity σ_{surf}. The remainder of the grid (L-χ_d) has the conductivity of σ_2 which is the free electrolyte conductivity in the pore space.

To accomplish this, one must know the surface conductivity σ_{surf} in the EDL. To quantitatively determine the surface conductivity at different rock-electrolyte interfaces is a complicated and non-trivial task (Pride, 1994; Schwartz et al., 1989; Waxman et al., 1968). The surface conductivity is related to both the rock microstructure and the saturating electrolyte salinity. One of the most famous electric conductivity models that accounts for the dual conductive pathways formed at pore brine and rock interfaces is described by the Waxman-Smits equation (Waxman et al., 1968),

$$\sigma_{\text{eff}} = \frac{1}{F}(\sigma_w + \frac{2\sigma_{surf}}{\Lambda}) = \frac{\sigma_w}{F}(1+X)\,. \qquad (6)$$

The Waxman-Smits equation divides the total effective conductivity of the fluid saturated porous medium into the contribution from electrolyte conductivity and the surface conductivity. In 2006, Devarajan quantitatively calculated the X in the Waxman-Smits equation, which equals to $\frac{2\sigma_{surf}}{\Lambda}$, with different values for the brine salinity, spatial distribution of clay minerals, rock structure and spatial fluid distribution in the pore space (Devarajan et al., 2006). The realistic values of X at low values of salinity vary from 1-10 depending on the rock type. At very high values of salinity, this ratio approaches zero (Devarajan et al., 2006). We can also calculate the value of Λ, which is the pore surface to pore volume ratio of our Fontainbleau Sandsotne CT image. Since our finite difference grid size is the same as the CT image voxel size, we can calculate the pore surface by the product of the number of grids that belong to the pore space and the surface area of the cubic grids. We can determine the pore volume from the product of porosity and the total 200^3 cubic volume which is $1mm^3$. The result we get for Λ is 10^5 m^{-1} for our Fontainbleau Sandsotne cube. This value is consistent

with the value obtained by Berryman in 1986 (Berryman et al., 1986). He calculated the pore surface to pore volume ratio over a wide porosity range and different types of sandstones using the two-point correlation function of the 2D digital images of rock samples. Our value is in within the range of his study.

After we determine the surface to volume ratio Λ in the Waxman-Smits equation, we can calculate the surface conductivity σ_{surf}. Assuming X=1for the Fontainbleau Sandstone saturated with low salinity electrolyte (say 10^{-3} S/m), we have

$$\frac{2\sigma_{surf}}{\Lambda} = \sigma_w X, \tag{7}$$

where σ_w is the free electrolyte conductivity σ_2 in our numerical model. By substituting Λ into the equation above, the surface conductivity is

$$\sigma_{surf} = \frac{\sigma_w \cdot \Lambda}{2}. \tag{8}$$

Next, we calculate the effective conductivity of the grid cells containing the surface conductivity σ_3 by the geometrically averaging across the grid cell. The effective conductivity is

$$\sigma_3 = \frac{\sigma_{surf} \cdot \chi_d + \sigma_2 \cdot (L - \chi_d)}{L} \approx 2 - 2.5\sigma_2. \tag{9}$$

where the ratio between the thickness of the EDL and the grid length ($\frac{\chi_d}{L}$) is 10^{-4}. This can be understood intuitively by taking the EDL and the free electrolyte in the grid to be two conductors in parallel. We can now add the third kind of grid cells with the EDL into our numerical model and calculate the effective conductivity with this three-phase conductivity model. The effective conductivity determined by the three-phase model is twice the conductivity by two-phase model. This result is consistent with the result from Waxman-Smits equation when we take the X as 1.

The formation factor can be calculated using Archie's Law. We superimpose the formation factor in another from the three-phase model on the result from the two-phase model in Fig 8. The three-phase result is much closer to the experiment data as indicated by the red square in Fig 11.

5. Conclusion

We develop a three-phase finite difference model to study the effect of surface conductivity on the effective conductivity of a 3D microstructure. We applied the finite difference code on a Fontainbleau Sandstone CT microtomographic image, which is a 200^3 volume of $1mm^3$ dimension. Many earlier works on this subject take the solid matrix to be an insulator with zero conductivity and fluid phase with unit conductivity to calculate the formation factor. We modified the finite difference code to solve the Laplace equation with different conductivity contrasts among the different phases. By doing this, we assigned physically realistic conductivity values for both the solid grain and saturated phases.

The effective conductivity and the current density distribution of Fontainbleau Sandstone saturated with gas, oil and different salinity brines are calculated. The numerically calculated formation factor of brine saturated sandstone using the two-phase model is almost 100% lower than the experimental data obtained by the previous work with samples of the same porosity. We re-discretize the CT image from a binary volume to a three phase volume by finding the boundary grids at the grain-pore space interface. We determine the surface conductivity in the EDL from the Waxman-Smits equation under different salinity conditions for the given geometric structure of our sample. By adding the third phase in our numerical model, the numerically calculated effective conductivity is much closer to the experimental data than the result from the two-phase model. This provides strong evidence for the importance of including surface conductivity into our numerical models.

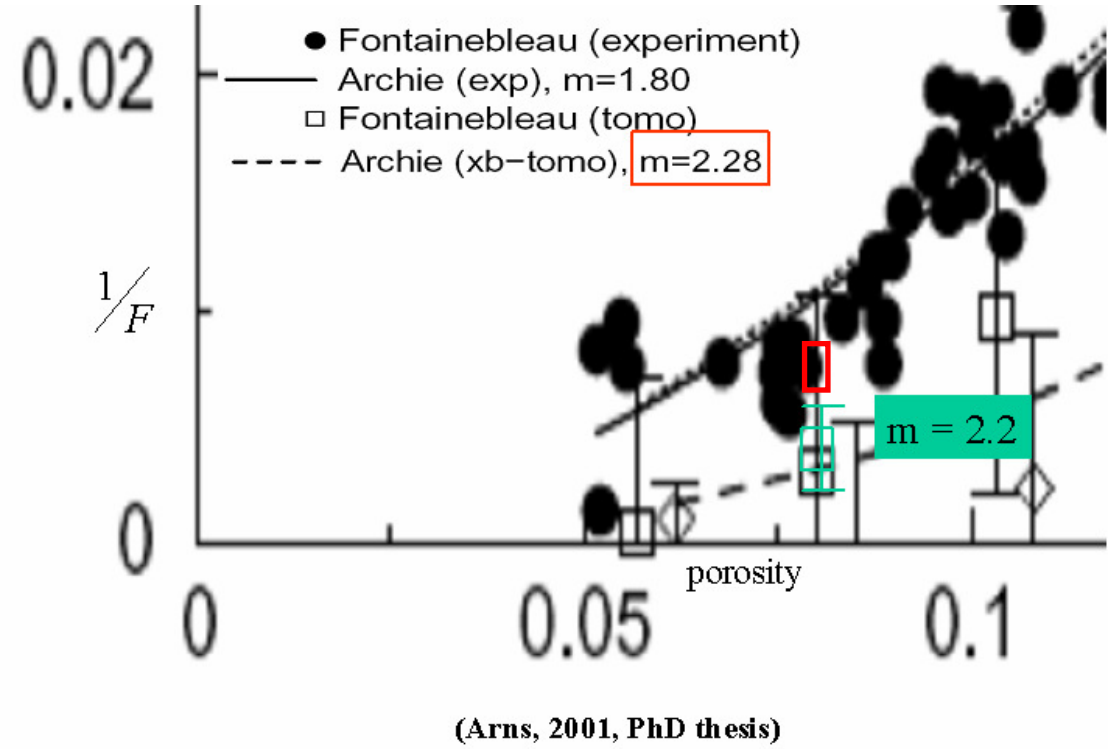

Figure 11: The comparison between two-phase result, three-phase result and the experiment measurements. The red square is the formation factor calculated from the three-phase model.

6. Acknowledgements

This work was supported by the Earth Resources Laboratory Borehole and Acoustic Logging Consortium and Founding Member Consortium.

References

Alder, P.M., Jacquin, C.G. and Quiblier, J.A.: 1990, Flow in simulated porous media, *Int. J. Multiphase Flow* **16,** 691-712.

Alder, P.M., Jacquin, C.G.. and Thovert, J.F.: 1992, The formation factor of reconstructed porous media, *Water Resour. Res.* **28**, 1571-1576.

Archie G.E.:1942, The electrical resistivity log as an aid in determining some reservoir characteristics, *Transactions of the American Institute of Mining, Metallurgy and Petroleum Engineers* **146**, 54–67

Arns, C. H.: 2001, The influences of morphology on physical properties of reservoir rock, *Ph.D. thesis, Univ. of New South Wales*.

Bentz, D. and Martys, N.: 1994, Hydraulic radius and transport in reconstructed model three-dimensional porous media, *Transport in Porous Media* **17,** 221-238.

Berryman, J.G and Blair, S.C.: 1986, Use of digital image analysis to estimate fluid permeability of porous material: Application of two-point correlation functions, *J.Appl.Phys* **60,** 1930-1938.

Bockris, J. and Reddy, A.K.N.: 2000, *Modern Electrochemistry*, Plenum Press, New York.

Coles, M. E., Spanne, P, Muegge, E.L. and Jones, K.W.: 1994, Computer microtomography of reservoir core samples, *Proc. 1994 Annual SCA Meeting,* Stavanger, Norway, Sept. 12-14.

Coles, M. E., Hazlett, R.D, Muegge, E.L. Jones, K.W., Andrews, B., Siddons, P., Peskin, A. and Soll, W.E.: 1996, Developments in synchrotron X-Ray microtomography with applications to flow in porous media, paper SPE 36531, *Proc. 1996 SPE Annual Technical Conference and Exhibition,* Denver, Oct 6-9.

Devarajan, S., Toumelin, E and Torres-Verdin, C.: 2006, Pore-scale analysis of the Waxman-Smits shaly sand conductivity model, SPWLA 47$^{th.}$ Annual Logging Symposium, June 4-7.

Garbozi, E.J.: 1998, Finite Element and Finite Difference Programs for Computing the Linear Electric and Elastic Properties of Digital Image of Random Materials, *NISTIR* **6269**.

Hazlett, R.D.: 1995, Simulation of capillary dominated displacements in microtomographic images of reservoir rocks, *Transport in Porous Media* **20,** 21-35.

Pal, E.R., Stig, B.: 2002, Process based reconstruction of sandstones and prediction of transport properties, *Transport in Porous Media* **46,** 311-343.

Pride, S. R. and Morgan, R. D.: 1991, Electrokinetic dissipation induced by seismic waves, *Geophysics*, **56**, 914-925.

Pride, S. R.:1994, Governing equations for the coupled electromagnetics and acoustic acoustics of porous media. *Phys. Rev. B* **50**, 15678-15696.

Revil, A. and Glover, P.W.: 1997, Theory of ionic-surface electrical conduction in porous media, *Physical Review B* **55,** 1757-1773.

Schwartz, L.M., Sen P.N and Johnson, D.L.: 1989a, Influence of rough surfaces on electrolytic conduction in porous media, *Phys. Rev. B* **40**, 2450-2458.

Waxman, M.H and Smits, L.J.M.: 1968, Electrical conduction in oil-bearing sands, *Society of Petroleum Engineers Journal*, **8**, 107-122.